frontiers in Chemical Engineering

ORIGINAL RESEARCH
published: 08 October 2020
doi: 10.3389/fceng.2020.00009

Original Method to Predict and Monitor Carbon Deposition on Ni-Based Catalysts During Dry Reforming of Methane

Rawaz Ahmed[1], *Takehiko Sasaki*[2] *and Maria Olea*[1]*

[1] School of Science, Engineering and Design, Teesside University, Middlesbrough, United Kingdom, [2] Graduate School of Frontier Sciences, The University of Tokyo, Tokyo, Japan

Although catalytic dry reforming of methane has recently attracted considerable attention from both environmental and economical points of view, due to the simultaneous utilization of two greenhouses with a high environmental impact, CO_2 and CH_4, and to the production of syngas (CO and H_2 mixtures), a building block used for the synthesis of valuable chemicals and synthetic fuels, it has not yet been commercialized. Low-cost Ni-based catalysts with high activity have been developed. However, due to their major drawbacks (such as carbon formation and Ni particles sintering at high temperatures, which is required by the endothermic reaction), their industrial applicability is limited. What is more, access to advanced characterization techniques is needed to monitor coke deposition and to assess the efficiency of the dry reforming process, access which can be challenging for small and on-site laboratories. The focus of this current study is on the development and testing of a simple carbon deposition prediction method, which is easily accessible, based on the comparison of the gas composition measured at the exit of the reactor with the theoretical one, and calculated based on the process thermodynamics. Trustworthy results, confirmed by SEM and TGA/DSC measurements, were obtained when the method was applied for the monometallic, Ni/SBA-15, prepared by wet impregnation, and bimetallic, Ni-Co/SBA-15, and Ni-La/SBA-15 samples, prepared by both impregnation and co-impregnation, with different metal loading. The dry reforming process was performed at four temperatures: 550, 600, 650, and 700°C.

Keywords: dry reforming of methane, Ni-based catalysts, precursors, nickel acetate, nickel nitrate, carbon deposition prediction, original method

OPEN ACCESS

Edited by:
Guanghui Zhang,
Dalian University of Technology, China

Reviewed by:
Zhenghong Bao,
Oak Ridge National Laboratory, United States
Zhuoran Xu,
BP North America Inc, United States

***Correspondence:**
Maria Olea
m.olea@tees.ac.uk

Specialty section:
This article was submitted to Catalytic Engineering, a section of the journal Frontiers in Chemical Engineering

Received: *25 January 2020*
Accepted: *30 July 2020*
Published: *08 October 2020*

Citation:
Ahmed R, Sasaki T and Olea M (2020) Original Method to Predict and Monitor Carbon Deposition on Ni-Based Catalysts During Dry Reforming of Methane. Front. Chem. Eng. 2:9. doi: 10.3389/fceng.2020.00009

INTRODUCTION

The transformation of biomass into valuable chemicals and fuels, using advanced processing methods and cutting-edge technologies, is becoming increasingly popular and challenging. Seen as a way to mitigate global warming and to diversify energy sources, the use of biomass for fuels, power production, and products that would otherwise be made from fossil fuels provides many benefits. The anaerobic digestion of biodegradable materials, such as livestock manure, food waste, municipal wastewater solids, fats, oils, and grease, to produce mainly biogas, 24 h a day, 7 days a week, is one of those advanced technologies. Refined processing of biogas via catalytic dry (or CO_2) reforming of methane (DRM) qualifies as a valuable route to produce syngas with a H_2/CO

ratio highly suited for the downstream conversion of biomass into long-chain hydrocarbons via the Fischer-Tropsch reaction.

The DRM process for syngas production involves a series of complex chemical reactions. The reactants ratio, the operational pressure, and temperature are important factors in generating a high yield of syngas without considerable side reactions that lead to undesired by-products. Besides the main reaction illustrated by Equation 1, there are several other series/parallel side reactions, which involve reactions between the reactants and the products of the DRM reaction. These side reactions include RWGS (Reverse Water Gas Shift) reaction (Equation 2), methane decomposition (Equation 3), CO disproportionation reaction or Boudouard reaction (Equation 4), and reverse carbon gasification reaction (Equation 5), as shown below (Tsai and Wang, 2008; Al-Fatish et al., 2009).

$$CH_4 + CO_2 \leftrightarrow 2H_2 + 2CO \quad \Delta H^o_{298} = 247kJ/mol(Dry\ reforming) \tag{1}$$

$$H_2 + CO_2 \leftrightarrow H_2O + CO \quad \Delta H^o_{298} = 41kJ/mol(Reverse\ water\ gas\ shift) \tag{2}$$

$$CH_4 \leftrightarrow C + 2H_2 \quad \Delta H^o_{298} = 75kJ/mol(Methane\ dissociation) \tag{3}$$

$$2CO \leftrightarrow CO_2 + C \quad \Delta H^o_{298} = -171kJ/mol(CO\ disproportionation) \tag{4}$$

$$CO + H_2 \leftrightarrow C + H_2O \quad \Delta H^o_{298} = -131kJ/mol(Reverse\ carbon\ gasification) \tag{5}$$

For the strongly endothermic reaction of dry reforming, the equilibrium conversion increases significantly with increasing reaction temperature. The equilibrium conversion of the moderate endothermic reactions, methane decomposition, and the reverse water-gas shift reaction also increase with temperature. The two carbon deposition reactions, the disproportionation reaction, and the reverse carbon gasification reaction are exothermic and thermodynamically unfavorable at high temperatures. Reaction temperatures above 750°C are required to reach a high equilibrium conversion value of CH_4 and CO_2 and to minimize the carbon formation through methane cracking and Boudouard reactions (Edwards and Maitra, 1995).

Group VIII B metals, like Co, Ni, Pt, Ru, Rh, and Ir, supported on alumina, titania, silica, or zirconia, were reported to show high catalytic activity in DRM reactions (Verykios, 2003); conversions approaching those defined by thermodynamics can be achieved as long as reaction temperature and contact time are sufficiently high.

However, as seen above, the major drawback of the DRM reaction is the coke formation which may cause catalysts' deactivation and clogging of the reactor. Although the noble metal-based catalysts provide lower carbon deposition in a DRM reaction than the Ni-based catalysts, their scarcity and high cost restrict their practicability. Therefore, recent studies on dry reforming of methane were focused on the development of Ni-based catalysts with high coking resistance and thermal stability (Arbag et al., 2016; Akri et al., 2019 and References herewith). Various methods, including the effect of supports Bradford and Vannice, 1999, the loading of metal San José-Alonso et al., 2013, the preparation method Xu et al., 2001, the use of promoters (Zhu et al., 2011) and the doping of other metals (Nikolla et al., 2007; Liu et al., 2009a,b), have therefore been investigated to improve the catalytic performance of Ni-based catalysts. It has been shown that the coke formation resistance of the Ni-based catalysts can be increased by adding alkali, alkaline, or lanthanide oxides or small amounts of noble metals, or by using the synergetic effect between Ni and Co. What is more, the preparation procedure for the bimetallic catalysts, such as co-impregnation or sequential impregnation, has significant effects on the resistance of carbon formation during the reaction (Erdogan et al., 2018).

Another significant factor influencing the catalytic performance and coke formation is the surface acidity of the supporting materials: the higher the surface acidity, the higher the amount of coke formed during dry reforming (Benrabaa et al., 2015). After the discovery of mesoporous silica (i.e., SBA-15, MCM-41) materials with ordered pore structures, studies on the synthesis of the mesoporous materials as catalyst support increased due to the elimination of the mass transfer limitation of reactants and/or products (Lin et al., 2002; Hukkamäki et al., 2004), andto the prevention of coke formation by their relative low surface acidity. (Huang et al., 2015), reported a superior performance of the SBA-15 supported bimetallic Ni-Co catalysts compared with that of monometallic catalysts in the dry reforming of methane.

To the best of our knowledge, there are no commercial DRM processes to date because of catalyst deactivation by coking and sintering of Ni species, although, as discussed above, considerable research effort has been put toward the developing of catalysts able to overcome these drawbacks. What is more, a thorough physical and chemical characterization of possible candidates, using advanced techniques, is required in order to select the best catalysts and to monitor their behavior during the DRM process. However, access to these techniques is rather challenging for small or on-site laboratories. Therefore, a simple method that does not require sophisticated techniques to monitor the carbon deposition over Ni-based catalysts during the dry reforming of methane process, at lab, pilot and, more importantly, at a commercial scale as well, when the commercialization will be fully operational, is of great demand.

Considering all these observations, the present study proposes an original method to predict the carbon deposition over monometallic and bimetallic Ni-based catalysts, supported on mesoporous silica, SBA-15, and attempts to contribute to the understanding of the carbon deposition process during the dry reforming of methane over these catalysts. The proposed prediction method has been successfully tested in the case of monometallic Ni/SBA-15 and bimetallic Ni-Co/SBA-15 and Ni-La/SBA-15 catalysts with increased metal loadings.

The authors would like to reiterate that the main aim of this paper was to share the original method which can be used to predict coke formation over different Ni-based catalysts, saving time and resources when testing a series of Ni-based catalysts in order to choose the one which, along with having rather

high activity, will not favor the coke deposition for the DRM process and not to systematically study the DRM reaction on the monometallic and bimetallic Ni-based catalysts.

Therefore, the results most significant and pertinent to this study, obtained by Ahmed (2013) (who performed a systematical study on Ni-based catalysts for DRM), with additional contribution on data analysis from the co-authors, were gathered and presented within this study, to support and to confirm the correctness of the proposed method.

MATERIALS AND METHODS

Preparation of SBA-15

The general experimental procedure followed in the preparation of mesoporous silica, via sol-gel method, was described in detail by Zhao et al. (1998a,b). This procedure was modified and the preparation conditions, such are the amount of P_{123}, type of acid, and aging time, were optimized through experiments (Ahmed, 2013). The optimized procedure is described below.

Therefore, 8 g of tri-block co-polymer of Poly (Ethylene oxide)-Poly (Propylene oxide)-Poly (Ethylene oxide) ($EO_{20}PO_{70}EO_{20}$, Pluronic P123) (Sigma-Aldrich) were added to 240 g of de-ionized (DI) water and kept at 40°C under stirring at ∼540 rpm for 6 h, until a clear solution was observed as a result of the complete mixing of P123 in water.

Then, 40 ml of HCl (37 wt%) (Fisher Scientific) was added to the dissolved P123 in water to reduce the pH of the solution and, ∼10 min later, 18.5 ml of Tetra Ethyl Ortho-Silicate (TEOS) (Sigma-Aldrich) was added dropwise in 25–30 drop/min to the solution under vigorous stirring. The solution was then kept under stirring at ∼540 rpm for hydrolysis and condensation reactions for 20 h. A white precipitate was formed which was transferred to an oil bath and kept at 95°C for 24 h to age without stirring. The white precipitate was then filtered, washed with ∼600 ml of DI water to remove the template (P123), and afterwards dried at 60°C for 24 h. The white powder was then calcined at 550°C under steady state conditions for 6 h. The heating rate was 10°C/min. Afterwards, 100 g of DI water was added to the calcined white powder in a round bottom flask and a short condenser inserted into the round bottom flask. The solution was then placed on a hot plate and left to boil for 2 h at 105°C with gentle stirring for surface hydration. After 2 h, the mixed solution was then filtered and a pure 4 g of SBA-15 sample was collected and dried at 120°C for 6 h.

Preparation of Monometallic Ni/SBA-15 Samples

The wet impregnation method was chosen for the preparation of the monometallic Ni-based samples. As precursors, nickel (II) acetate tetra-hydrate [$Ni(CH_3COO)_2.4H_2O$ (99%), average molecular weight 248.86] and nickel (II) nitrate hexa-hydrate [$Ni(NO_3)_2.6H_2O$ (99%) (Sigma-Aldrich) were used. DI water was used throughout the experiments.

The impregnation was carried out at different temperatures, for different impregnation times and different impregnation treatments. Samples were prepared and labeled, as shown in **Table 1**.

The impregnation temperature was higher for nickel acetate than for nickel nitrate because of its lower solubility in water. For example, at 20°C, the solubility of nickel nitrate is 94 g/100 ml in water, while for nickel acetate the solubility is only 17 g/100 ml. The calcinations temperature was chosen as 550°C, because at too low a temperature (e.g., 200°C), the nickel salt does not have a complete decomposition to form NiO, whereas at too high a calcination temperature (e.g., 800°C), the sintering and /or fusing of nickel active sites through the annealing effects can occur (Steinhauer et al., 2009). Therefore, all samples were calcined in air atmosphere at 550°C, for 2 h, at a heating rate of 10°C/min.

Preparation of Bimetallic Ni-Metal/SBA-15 Samples (Me = Co and La)

For the preparation of the bimetallic samples, both the sequential and co-impregnation methods were employed, using lanthanum (III) nitrate hexa-hydrate [$La(NO_3)_3\ 6H_2O$, (99.99%), average molecular weight 433.01], cobalt (II) nitrate hexa-hydrate [$Co\ (NO_3)_2\ 6H_2O$ (98%), average molecular weight 291.03], and cobalt (II) acetate tetra-hydrate [$Co\ (CH_3COO)_2.4H_2O$ (98.00%), average molecular weight 249.08] as precursors. The following samples were prepared and labeled as shown in **Table 2**.

TABLE 1 | Preparation conditions and labels for the monometallic Ni/SBA-15 samples.

Precursor	SBA-15:Ni-salt: DI water (wt ratio)	IMP. Time (h)	Heat treatment		Label* XIMPNi
			IMP. Temp (°C)	Drying	
Ni-acetate	3:1:10	10	90–95	dried at 120°C, 10 h	4IMPNiA-A
	3:2:10				9IMPNiA-B
	3:3:10				12IMPNiA-C
Ni-nitrate	3:1:10	10	50–55	dried at 120°C, 10 h	6IMPNiN-A
	3:2:10				12IMPNiN-B
	3:3:10				29IMPNiN-C

**X is the wt% of nickel loaded as NiO, determined from EDX, IMP refers to impregnation, NiA, Ni-acetate; NiN, Ni-nitrate.*

TABLE 2 | Preparation conditions and labels for the bimetallic Ni-Metal/SBA-15 samples.

Precursor	IMP. Time = 1–2 h, Temp = 50–60°C	Heat-treatment		Precursor	IMP. Time = 1–2 h, Temp = 50–60°C	Heat-treatment		Label**
	SBA-15: Co or La : DI water (wt ratio)	Drying*	Calc.		Samples: Ni: DI water (wt ratio)	Drying*	Calc.	
Sequential impregnation method								
Co-acetate	1:0.33:10	100°C, 1 h	400°C, 5 h, 10°/min	Ni-acetate	0.78:0.78:10	100°C, 1 h	650°C 4 h, 10°/min	9 IMPNi2CoA-A
	1:0.67:10				0.85:1.5:10			15IMPNi4CoA-B
	1:1:10				0.96:2:10			16IMPNi8CoA-C
La-nitrate	2:0.67:20	100°C, 1 h	550°C, 2 h, 5°/min	Ni-nitrate	1.77:1.52:18	100°C, 1 h	550°C, 2 h,5°/min	10IMPNi6LaN-A
	2:1.33:20				1.9:2:18.9			13IMPNi18LaN-B
	2:2:20				1.87:2.5:18.7			16IMPNi11LaN-C

Co-impregnation method

Precursor	SBA-15: Co or La :Ni :DI water (wt ratio)	IMP. Time & Temp	Heat-treatment		Label**
			Drying*	Calc.	
Co-nitrate Ni-nitrate	1:1.33:1.33:10	1–2 h, 40–50°C	100°C, 1 h	550°C, 5 h, 5°/min	12COIMPNi11CoN-C
La-nitrate Ni-nitrate	1:0.67:0.67:10	1–2 h, 40–50°C	100°C, 1h	550°C, 5 h, 5°/min	4COIMPNi12LaN-B

vacuum oven; Calc, Calcination.

*** The samples were labeled as follows. For those obtained by the sequential impregnation method, XIMPNiYCoA-A, B, and C or XIMPNiYLaN-A, B, and C, where, IMP, Impregnation; X, nickel loading; Y, Co or La loading; as determined through EDX measurements, A, Ni-acetate or Co-acetate as precursors; N, Ni- nitrate or La-nitrate as precursors; and A, B, and C refers to the initial concentration of the precursor solution. As for those obtained by co-impregnation, the "IMP" in the label was replaced by "COIMP".*

Original Method to Predict the Carbon Deposition

The method is based on the results obtained while measuring the catalytic activity of the monometallic and bimetallic Ni-based samples toward the DRM reaction, by using a CATLAB system (Hiden Analytical, UK). The system comprises the Hiden Analytical *QIC-20* dynamic sampling mass spectrometer (MS) and the CATLAB microreactor module with the units seamlessly integrated to provide one of the most versatile and accurate catalysts' characterization system available.

The below procedure to convert the voltage signal of the MS into partial pressure was followed.

The amplifier in the detector measures the ion flow on the Faraday cup. This is then converted using the 1 × 10e-4A/torr or 1 × 10e-4A/mbar, depending on which pressure units are used within the RC interface.

This is a calibration factor that has been pre-determined as the average sensitivity of Hiden Analytical products.

When an instrument is tested in production, it is tested to this spec to ensure it measures close to this performance.

At the beginning of the measurements, the fragmentation patterns for each of the gases were measured. Since fragments of different products can occur on the same AMU's, care should be taken when ascribing an AMU to a certain product. Therefore, the species of interest were admitted over a reactor filled with inert particles and catalyst particles, respectively. Comparison of both spectra gave an indication about which AMU's can be ascribed to reactants or products. Moreover, if different products appear on the same AMU, the fraction of each at that respective AMU could be determined and later subtracted for an accurate value of the partial pressure of the species of interest.

The fragmentation peaks can also be found online at NIST Mass Spectrometry Data Center (http://webbook.nist.gov/chemistry/).

When CO_2 was measured at AMU 44, as the other present species did not have a fragmentation peak at AMU 44, we considered its partial pressure as it was read.

When CO was measured at AMU 28, the contribution to the signal from the CO_2 fragmentation pattern (which was about 10%, similar to that from NIST) was subtracted from the response.

Thus, the CO_2 reforming of the methane reaction was conducted under atmospheric pressure and constant temperature, namely 550, 600, 650, and 700°C, respectively, in the CATLAB system. About 25 mg of each sample was firstly reduced under a 5 vol. % H_2 in Ar flow at 20 ml/min and

then exposed to the reaction mixture of 100 ml/min flow, with $CH_4/CO_2 = 1.5{:}1$, for 3 h.

The choice of reaction time of 3 h was based on the following judgment. As mentioned in this study, there are no commercial DRM processes to date, due to catalyst deactivation by coking and to the sintering of Ni species. Both deactivation processes impact significantly into the lifetime of the catalysts. It is well-known that the determination of catalytic activity, selectivity, and lifetime of industrial catalysts is an expensive and time-consuming task. Therefore, accelerated testing procedures are foreseen. As such, preliminary testing of the sample, which was more prone to coke deposition, i.e., 29IMPNiN-C, for different time-on-stream, up to 50 h, was performed. It was observed from TGA/DSC that the amount of carbon deposited stays constant after 3 h.

The analysis of the effluent was carried out using the quadruple mass spectrometer, *QIC-20*. The following amus were measured: 2 (H_2), 40 (Ar), 18 (H_2O), 15 (CH_4), 28 (CO), 32 (O_2), and 44 (CO_2). As mentioned above, the integrated software allowed the conversion of intensity of the amu into the pressure and as such, in this work, the conversions, *X*, of the limiting reactant, CO_2, was calculated according to the following equation:

$$X_{CO_2} = \frac{P^o_{CO_2} - P_{CO_2}}{P^o_{CO_2}} * 100 \tag{6}$$

Moreover, assuming that only the reforming reaction occurred, the theoretical pressure of methane leaving the reactor was calculated according to the following equation and was compared with the measured methane pressure. Then, the difference, Δ, between the two values was calculated.

Theoretically,

$$P_{CH_4\,T} = P^o_{CO_2}\left(1.5 - X_{CO_2}\right) \quad and \quad \Delta = P_{CH_4\,T} - P_{CH_4} \tag{7}$$

where, $P^o_{CO_2}$ is the initial pressure of CO_2 and X_{CO2} is the CO_2 fractional conversion, while P_{CH_4} and P_{CO_2} are the pressure of CH_4 and CO_2, respectively, leaving the reactor.

The coke is formed only if the side reactions 3, 4, and 5 occur, as shown above. However, from a thermodynamic point of view, only reaction 3 is probable at the reaction temperatures (reaction 3 is endothermic, while 4 and 5 are strongly exothermic) (See **Supplementary materials** for Thermodynamics calculations).

TABLE 3 | Calculated compared with measured methane pressure (leaving the microreactor) and CO_2 conversion for the monometallic Ni/SBA-15 catalyst samples at 550, 600, 650, and 700°C, respectively.

Catalysts	T (°C)	X_{CO2} (%)	Calculated P_{CH4} (Torr)	Experimental P_{CH4} (Torr)	Δ Value (Torr)
4IMPNiA-A	550	65	1.04E-09	1.66E-09	−6.19E-10
	600	90	3.24E-10	9.27E-10	−6.03E-10
	650	97	1.15E-10	5.78E-10	−4.68E-10
	700	100	5.50E-11	1.89E-10	−1.34E-10
9IMPNiA-B	550	80	3.98E-10	9.50E-10	−5.52E-10
	600	88	2.59E-10	7.22E-10	−4.63E-10
	650	100	1.68E-10	3.77E-10	−2.09E-10
	700	100	1.10E-10	1.58E-10	−4.72E-11
12IMPNiA-C	550	79	4.71E-10	1.15E-09	−6.79E-10
	600	86	1.46E-10	6.49E-10	−5.03E-10
	650	98	5.65E-11	5.28E-10	−4.71E-10
	700	100	1.10E-10	3.76E-10	−2.67E-10
6IMPNiN-A	550	69	3.07E-09	1.66E-09	1.41E-09
	600	87	1.36E-09	4.87E-10	8.68E-10
	650	96	3.01E-09	6.04E-10	2.40E-09
	700	94	2.18E-09	3.67E-10	1.81E-09
12IMPNiN-B	550	77	2.53E-09	1.21E-09	1.31E-09
	600	92	2.58E-09	1.03E-09	1.55E-09
	650	96	1.57E-09	4.26E-10	1.15E-09
	700	100	2.87E-09	7.12E-10	2.16E-09
29IMPNiN-C	550	76	2.67E-09	9.02E-10	1.77E-09
	600	94	2.10E-09	6.12E-10	1.49E-09
	650	98	2.83E-09	4.86E-10	2.34E-09
	700	97	1.93E-09	3.67E-10	1.56E-09

Therefore, let us consider that if coke is formed, it is formed through reaction 3 only. But, if there is no coke formed over the catalysts, only reaction 1 and 2 should have occurred. As reaction 1 is more endothermic than reaction 2, one can assume that mainly only reaction 1 occurred. If this is the case, the value for Δ, as defined above, should be, if not zero, a very small negative one. Following the same reasoning, if coke is formed, Δ should have a positive value.

Although the method was developed using the mass spectrometry results, it can be applied to other techniques which allow the measurement of the exit gas composition (such as gas chromatography, Raman spectroscopy, and Fourier transform infrared spectrometry).

RESULTS

Monometallic Ni/SBA-15 Samples

Table 3 presents the calculated and experimentally-measured methane pressure values at the exit of the microreactor, along with their difference, and the carbon dioxide conversion at four temperatures, i.e., 550, 600, 650, and 700°C, respectively, for the monometallic Ni/SBA-15 samples. The difference between the two pressure values is negative for the samples for which the nickel acetate was used as precursor, while for the samples prepared by using nickel nitrate as nickel precursor during impregnation the difference is positive.

If the proposed procedure is correct, then there should not be any coke formation during the DRM reaction over the catalysts prepared with nickel acetate, while the coke formation is expected over those catalysts prepared by using nickel nitrate as precursor.

Although nickel nitrate is the nickel precursor generally selected to prepare oxide-supported catalysts due to its low

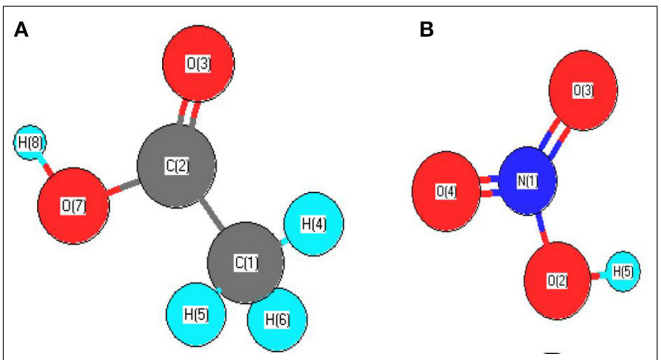

FIGURE 2 | (A) Geometry structure of acetic acid; **(B)** Geometry structure of nitric acid (Ahmed, 2013).

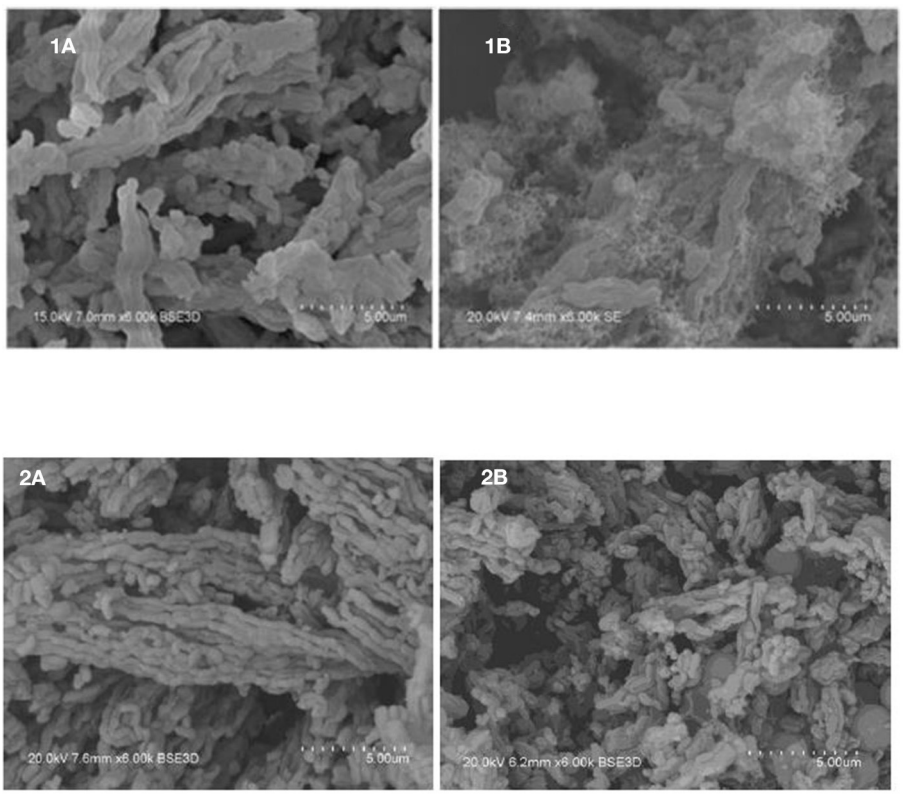

FIGURE 1 | SEM images of **(1A)** 9IMPNiA-B and **(1B)** 12IMPNiN-B spent catalysts (550°C). SEM images of **(2A)** 9IMPNiA-B and **(2B)** 12IMPNiN-B fresh catalysts.

cost, high solubility in water, and decomposition at moderate temperatures, there are disadvantages in using it as a precursor. Its decomposition produces non-stoichiometric nickel oxide (NiOx) and it is known to melt and redistribute over the supporting material, leading to poorly dispersed metal particles after reduction and to their partial expulsion from the porous support system (Marceau et al., 2010). By using nickel acetate as a precursor, all these disadvantages are avoided.

The wide-angle XRD spectra showed that, for samples prepared with nitrate as precursor, the average NiO particle size was 10.0 nm, while for those prepared with concentrate nickel acetate solution (sample 12IMPNiA-C), the average NiO particle size was 8.0 nm. When diluted nickel acetate solution was used (sample 9IMPNiA-B), only very weak and broad reflection peaks are observed, indicating that exclusively uniformly dispersed, very small nickel oxide particles are formed (Ahmed, 2013).

In order to support these statements, SEM was performed on the fresh and spent catalysts samples discussed in **Table 3**. **Figure 1** presents, comparatively, the SEM images obtained over the 9IMPNiA-B and 12IMPNiN-B spent catalyst samples **Figures 1(1A,B)** and fresh samples **Figures 1(2A,B)**, respectively. Although both samples were prepared using the same SBA-15:Ni-salt:DI water weight ratio, increased Ni loading was observed when nitrate was the precursor. At the same time, it was noticed that the dispersion of the NiO species on the surface of the support, SBA-15, decreased by increasing the loading (Ahmed, 2013). The difference in dispersion can be explained by taking into account the size and geometry of acetic acid against the size and geometry of nitric acid (see **Figure 2**).

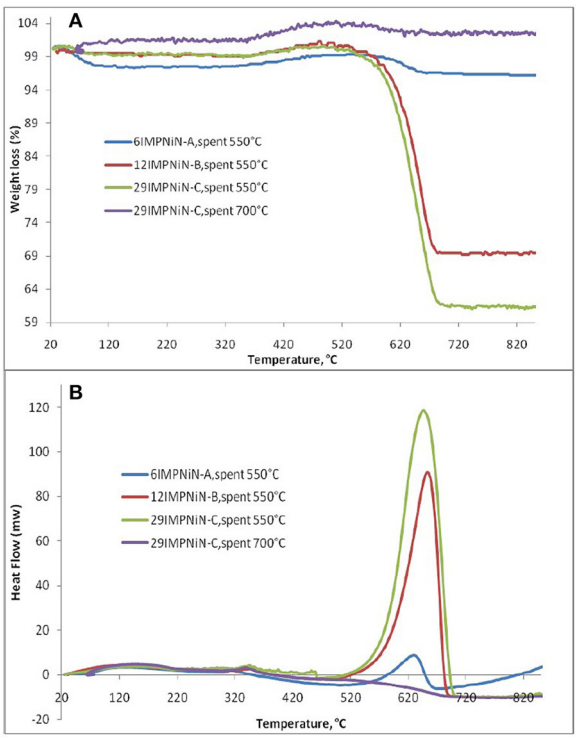

FIGURE 4 | TGA **(A)**/DSC **(B)** analysis of: 6IMPNiN-A spent at 550°C, 12IMPNiN-B spent at 550°C, 29IMPNiN-C spent at 550°C, and 29IMPNiN-C spent at 700°C samples.

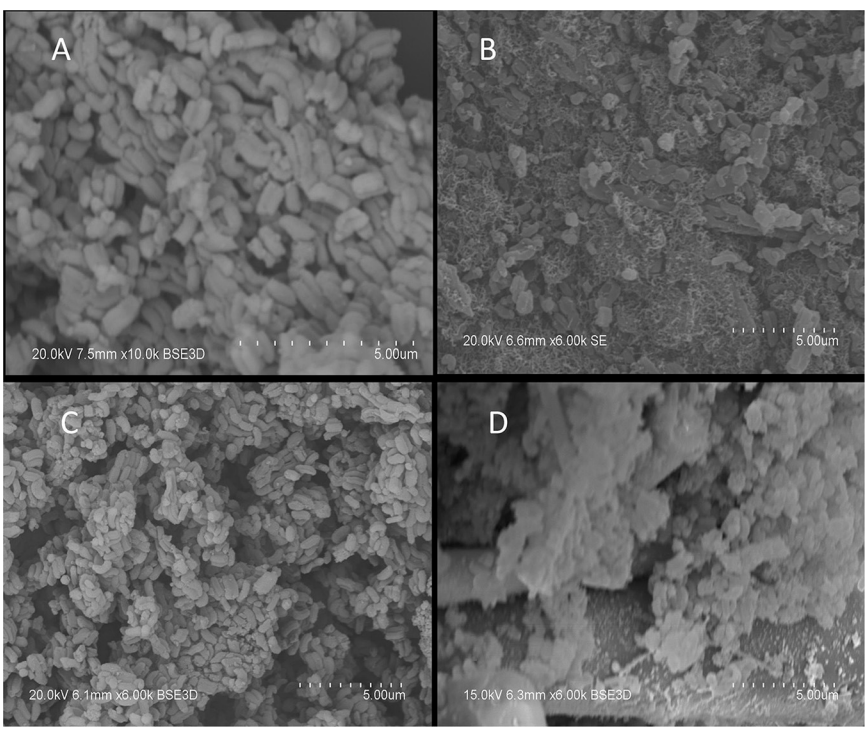

FIGURE 3 | SEM images of 6IMPNiN-A [**(A)** fresh and **(B)** spent, 550°C] and 29IMPNiN-C [**(C)** fresh and **(D)** spent, 550°C] catalysts.

As the first one is a bigger molecule, it will favor the dispersion of Ni species on the support; as the second one is a smaller molecule, it will favor more Ni loading on the SBA-15 supports with the same BET surface area. Moreover, the nature of the precursor influenced the structure of the reduced species as well. Wide-angle XRD taken after reduction showed the nickel metallic species was well-dispersed for the samples prepared with nickel acetate (their size was assumed to be <3 nm, as no reflection peaks were detected), while in the case of the samples prepared with nickel nitrate, nickel clusters were obtained after reduction. Their size increased from 8 to 20 nm as the Ni loading increased from 6 to 29 wt%, respectively (Ahmed, 2013).

As predicted, there is no coke formation observed on the nickel acetate sample, while there is a considerable amount of coke formed during the dry reforming of methane reaction over the nickel nitrate catalyst sample.

Figure 3 presents, comparatively, the SEM images taken over two ex-nitrate samples, both fresh and spent 6IMPNiN-A and 29IMPNiN-C samples, respectively. As predicted, there is coke formation over the spent catalyst samples. The amount of coke seems to increase with the increasing of the Ni loading; the particles are completely covered with carbon for the 29 wt% Ni loading.

Furthermore, to determine the amount of carbon formed on the surface, the spent ex-nitrate catalysts were analyzed by using TGA/DSC. **Figure 4A** shows only one significant weight loss in the 550–695°C range, which is due to the combustion of coke deposited on the catalyst. Besides the weight loss, a slight weight

TABLE 4 | Calculated compared with measured methane pressure (leaving the microreactor) and CO_2 conversion for the bimetallic Ni-M/SBA-15 catalyst samples (M = Co and La) (prepared by sequential impregnation and co-impregnation), at 550, 600, 650, and 700°C, respectively.

Catalysts	T (°C)	X_{CO2} (%)	Theoretical, P_{CH4} (Torr)	Practical, P_{CH4} (Torr)	Δ-value (Torr)
9IMPNi2CoA-A	550	74	5.82E-10	1.09E-09	−5.11E-10
	600	89	4.68E-10	8.92E-10	−4.24E-10
	650	95	3.51E-10	3.72E-10	−2.07E-11
	700	100	5.40E-11	2.63E-10	−2.09E-10
15IMPNi4CoA-B	550	70	8.06E-10	1.10E-09	−2.91E-10
	600	90	2.84E-10	8.49E-10	−5.65E-10
	650	95	5.83E-11	3.63E-10	−3.04E-10
	700	100	1.64E-10	3.48E-10	−1.84E-10
16IMPNi8CoA-C	550	85	3.68E-10	1.18E-09	−8.13E+10
	600	94	3.44E-10	8.30E-10	−4.84E-10
	650	100	2.84E-10	4.66E-09	−1.83E-10
	700	100	1.10E-10	3.63E-10	−2.53E-10
10IMPNi6LaN-A	550	41	3.46E-09	2.36E-10	3.23E-09
	600	89	9.50E-10	8.10E-10	1.41E-10
	650	96	3.44E-10	2.64E-10	8.07E-11
	700	100	5.66E-10	4.34E-10	1.32E-10
13IMPNi18LaN-B	550	80	2.64E-09	1.13E-09	1.51E-09
	600	85	2.74E-09	1.10E-09	1.65E-09
	650	100	9.88E-10	2.28E-10	7.59E-10
	700	100	1.35E-10	3.70E-10	9.80E-10
16IMPNi11LaN-C	550	75	4.92E-09	1.14E-09	3.78E-09
	600	91	2.24E-09	6.35E-10	1.60E-09
	650	98	1.12E-09	2.87E-10	8.36E-10
	700	96	7.93E-10	3.47E-10	4.46E-10
12COIMPNi11CoN-C	550	77	5.82E-10	4.22E-10	1.59E-10
	600	83	6.43E-10	4.29E-10	2.13E-10
	650	96	4.03E-10	2.17E-10	1.86E-10
	700	100	6.55E-10	1.79E-10	4.76E-10
4COIMPNi12LaN-B	550	64	1.30E-09	8.16E-10	4.98E-10
	600	81	1.20E-09	5.76E-10	6.36E-10
	650	92	7.08E-10	2.10E-10	4.97E-10
	700	100	4.90E-10	1.50E-10	3.43E-10

gain caused by the oxidation of metallic Ni particles was also observed. The higher the Ni loading, the higher the amount of coke deposited for the spent samples in the DRM reaction at 550°C. There was a 2.8% weight loss for the 6IMPNiN-A spent sample. For the 12IMPNiN-B spent sample, the weight loss was 30.5%, while for the 29IMPNiN-C spent catalyst the weight loss was 37.9%. But almost no weight loss was observed for the used samples in the reaction run at 700°C. This is an expected result as at higher reaction temperatures the carbon gasification side reaction can occur as well. The DSC curves (see **Figure 4B**) of the samples show two exothermic peaks: (i) a small one at lower temperatures, which can be assigned to the oxidation of metallic nickel to Ni^{2+}; and (ii) a strong one at higher temperatures which is due to the gasification of carbon. As the DSC curves present only one strong exothermic peak, one can conclude that only one kind of carbonaceous species was deposited on the surface of these catalysts, most likely graphite-like carbon (Guczi et al., 2010; result supported by the XRD measurements and by Ahmed, 2013).

In addition, to explain why almost no coke formation was observed at 700°C, we assumed that at a higher reaction temperature the carbon gasification side reaction can occur as well. Ahmed (2013) performed the Temperature Programmed Oxidation reaction over the spent catalysts.

As the TPO results have shown, a broad but low intensity CO_2 peak, centered around 650°C, was observed for the 29IMPNiN-C sample. This means that some strongly bonded carbon species were deposited during the DRM reaction. As for the XRD results, they were graphite species (Guczi et al., 2010). (Even lower amounts of carbon were formed on the other two Ni ex-nitrate samples, but they were not detectable by TPO). No CO_2 peaks were observed for the Ni ex-acetate catalysts. What was more, in

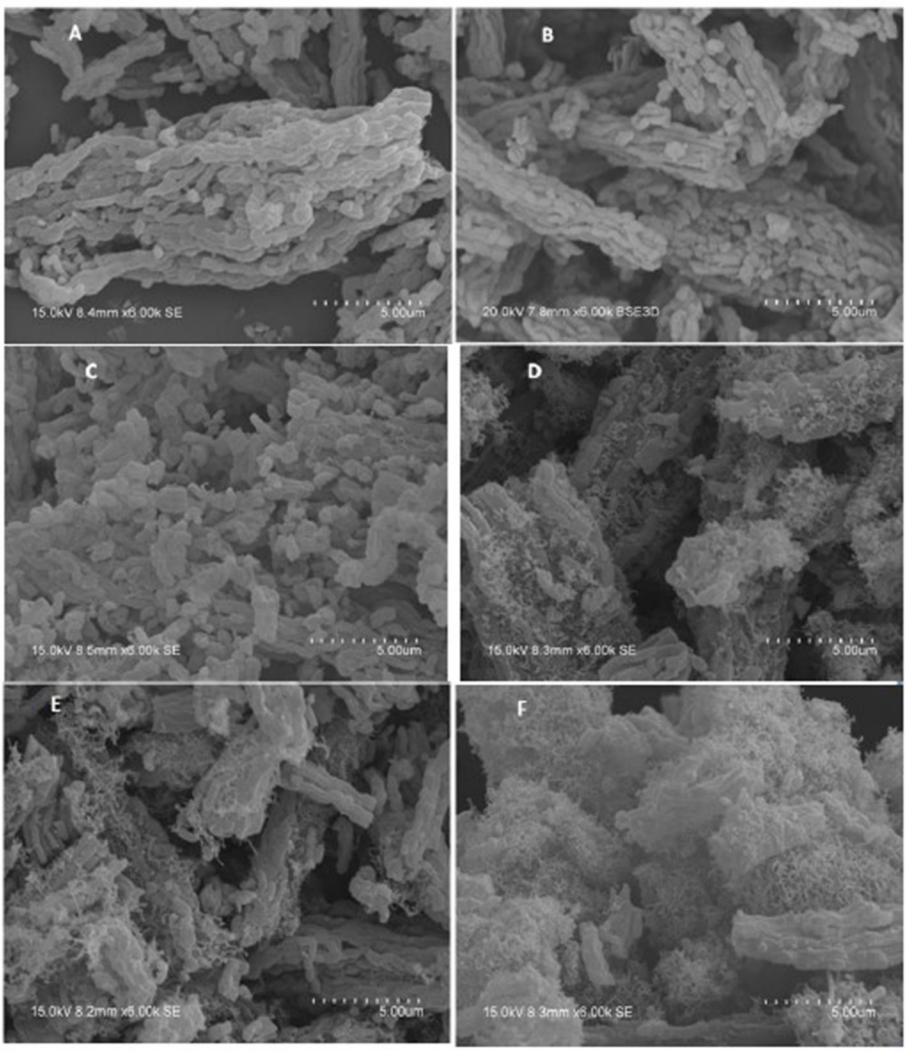

FIGURE 5 | SEM images of **(A)** 9IMPNi2CoA-A, **(B)** 15IMPNi4CoA-B, **(C)** 16IMPNi8CoA-C, **(D)** 10IMPNi6LaN-A, **(E)** 13IMPNi18LaN-B, and **(F)** 16IMPNi11LaN-C spent samples at 550°C.

this TPO experiment, there was no signal for water, which was in line with previous work (Liu et al., 2009b).

One can conclude that the size of the Ni particles, which in turn depends on the nature of the nickel precursor and nickel loading, is responsible for their resistance toward carbon formation: the smaller the size, the higher the resistance.

Our results confirmed the importance of minimizing the Ni particle size in minimizing the coke deposition on Ni-based catalysts, as carbon deposition on an Ni surface is known to necessitate Ni ensembles, and large Ni particles cause more severe coke deposition (Han et al., 2017 and References herewith). Theoretical studies revealed that if the Ni facets or step edges were small enough, which was the case for nickel particles <10 nm, nucleation of graphene could not proceed and graphite formation was further suppressed (Bengaard et al., 2002). Olea et al. (2014), proposed an optimized method to deposit well-dispersed Ni particles into SBA-15 mesoporous silica, to avoid coke deposition and sintering as well. Also, our results are in line with published results on nickel-grafted SBA-15 by Liu et al. (2009b), which confirmed that the highest catalytic activity and long-term stability were obtained over a 5 wt.% Ni/SBA-15 catalyst, with Ni species well-dispersed into the high surface area of SBA-15. This superior catalytic behavior was closely related with the strong resistance toward carbon formation and active metal sintering.

There is another important factor which contributes to the stability of the Ni-based catalysts. As the dry reforming reaction typically occurs at very high temperatures, the initially small Ni particles become sintered and the size of the Ni domains eventually becomes large with heavy coke deposition. Strong metal-support interactions are often used to maintain the small size of the Ni particles at high reaction temperatures. A way to quantify the metal-support interactions is to study the kinetics of the H_2-reduction of the calcined samples. Ahmed (2013), found that for the catalysts prepared using nickel nitrate as precursor that the activation energy for the reduction process decreased as the Ni-loading increased, which means that the metal-support interaction is stronger at lower Ni loading. Accordingly, less carbon deposition should occur on the catalysts with lower Ni loading as compared with those with higher loading. Our TGA results support this statement.

Bimetallic Ni-Metal/SBA-15 Samples (Me = Co and La)

Table 4 presents the calculated and the experimentally measured methane pressure values at the exit of the microreactor along with their difference, and carbon dioxide conversion at four temperatures, i.e., 550, 600, 650, and 700°C, respectively, for the bimetallic Ni-M/SBA-15 samples, prepared by both impregnation and co-impregnation. As stated above, if Δ, the difference between the two pressure values, was zero or a very small negative value, then no carbon formation was expected over that catalyst. In contrast, when Δ was positive, some carbon formation is expected. Therefore, one can conclude that the Ni-Co catalysts prepared by sequential impregnation would not favor the carbon deposition during the DRM reaction, while the sequential impregnated Ni-La samples and those obtained by co-impregnation would favor the coke formation. To confirm this statement, TGA/DSC and SEM measurements were performed over the spent catalysts in order to assess the carbon formation. **Figures 5A–F** shows the SEM morphologies of spent (at 550°C) Ni-Co and Ni-La samples, obtained by sequential impregnation. There was no carbon deposition observed over all the Ni-Co catalysts, not even for the highest Ni-Co loading sample (i.e., 16IMPNi8CoA-C). By contrast, some carbon deposited over the Ni-La catalysts was observed. The maximum amount of carbon deposited seems to be on the 16IMPNi11LaN-C sample. This observation was confirmed by the TGA measurements.

Figure 6A shows only one significant weight loss in the 550–695°C temperature range, which is due to the combustion of coke deposited on the catalyst. Besides the weight loss, a slight weight gain caused by the oxidation of metallic particles was also observed. There was a 7.8 wt% of weight loss for

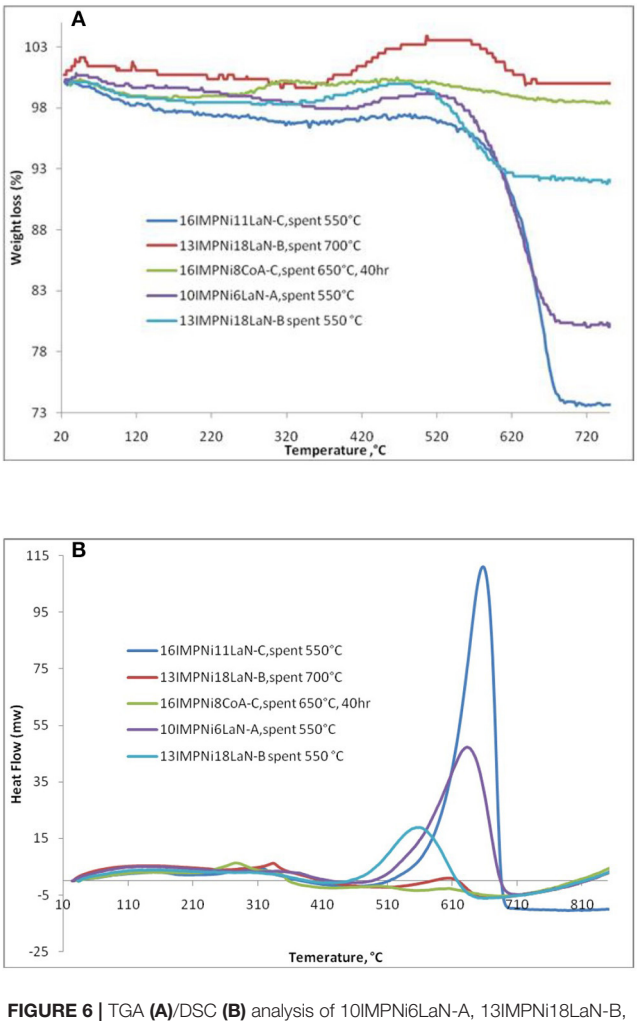

FIGURE 6 | TGA **(A)**/DSC **(B)** analysis of 10IMPNi6LaN-A, 13IMPNi18LaN-B, 16IMPNi11LaN-C, and 16IMPNi8CoA-C spent samples.

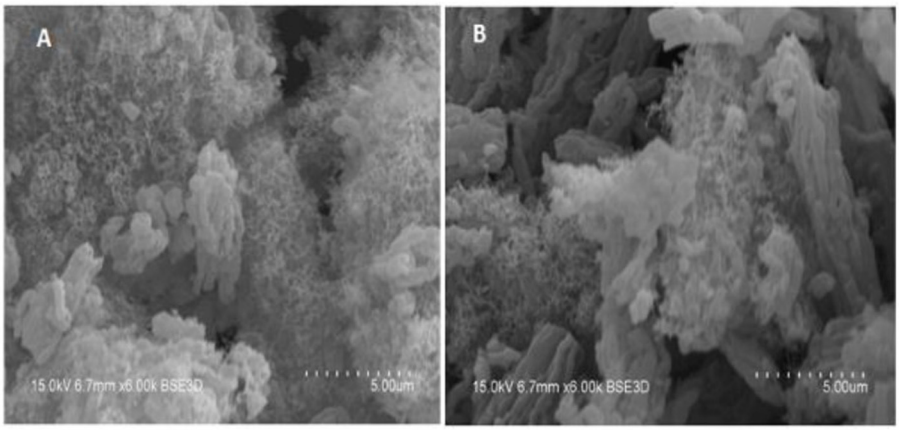

FIGURE 7 | SEM images of 12COIMPNi11CoN-C **(A)** and 4COIMPNi12LaN-B **(B)** samples after reaction at 550°C.

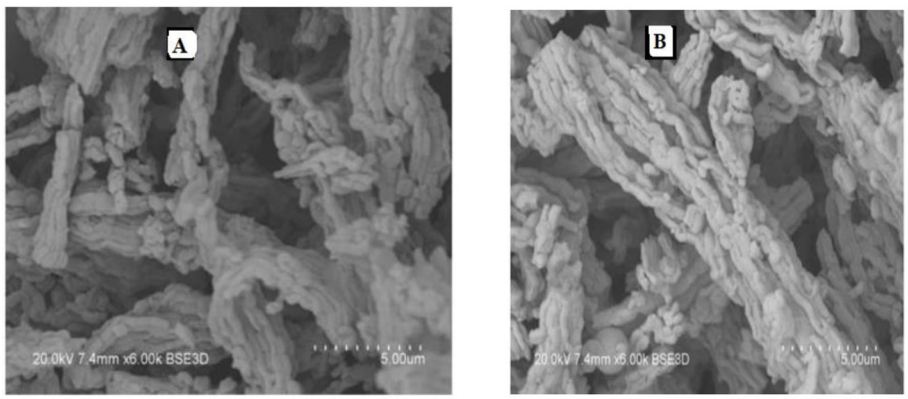

FIGURE 8 | SEM images of fresh samples 12COIMPNi11CoN-C **(A)** and 4COIMPNi12LaN-B **(B)**.

the 13IMPNi18LaN-B spent sample. For the 10IMPNi6LaN-A spent sample, the weight loss was 19.0 wt%, while for the 16IMPNi11LaN-C spent catalyst the weight loss was 22.4 wt%. But almost no weight loss was observed for the used samples in the reaction run at 700°C. This is an expected result again as at higher reaction temperatures the carbon gasification side reaction can also occur. On the other hand, no weight loss was observed for all Ni-Co catalysts over 40 h time on stream (only 16IMPNi8CoA-C samples after reaction for 40 h, shown here), indicating that the additional Co component in the catalyst had a great beneficial effect on the catalyst performance without carbon formation on the surface of the catalyst.

The DSC curves (see **Figure 6B**) of the samples show two exothermic peaks: (i) a small one at lower temperatures which can be assigned to oxidation of metallic nickel to Ni^{2+}; and (ii) a strong one at higher temperatures, which is due to the gasification of carbon. As the DSC curves present only one strong exothermic peak, one can conclude that only one kind of carbon was deposited on the surface of these catalysts, most likely graphite-like carbon (Guczi et al., 2010; result supported by the XRD measurements as well, Ahmed, 2013).

There was some change in the intensities of the peaks for all samples, likely due to the different size of metal particles. The intensity of the DSC peaks gradually decreased with La content from the 10IMPNi6LaN-A to the 13IMPNi18LaN-B samples. This means that La actually played dual roles in preventing the carbon formation for the CO_2 reforming of CH_4. On the one hand, the basic La_2O_3 favored the chemisorption and dissociation of CO_2 and subsequently accelerated the carbon elimination by $CO_2 + C \rightarrow 2CO$. On the other hand, the La dispersed in the SBA-15 and Ni crystallites could prevent the Ni grains from excessive growth at high temperatures.

Figure 7 presents the SEM results over the 12COIMPNi11CoN-C and 4COIMPNi12LaN-B spent samples. If these results are compared with those obtained over the fresh catalysts as presented in **Figure 8**, one can say that there is carbon deposition over both co-impregnated spent samples, Ni-Co and Ni-La.

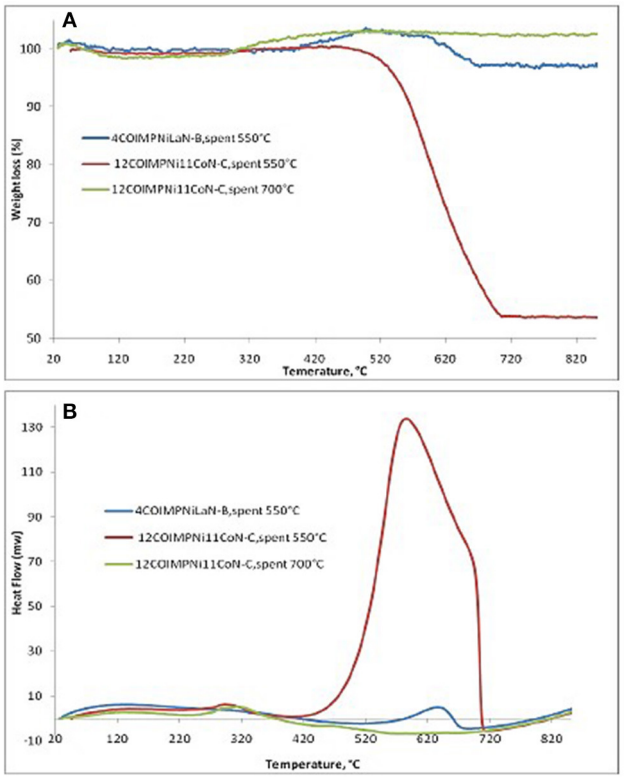

FIGURE 9 | TGA **(A)** and DSC **(B)** analysis of 12COIMPNi11CoN-C and 4COIMPNi12LaN-B spent samples.

Furthermore, to determine the amount of carbon formed on the surface of spent co-impregnated catalysts, TGA/DSC measurements were performed. **Figure 9A** shows only one significant weight loss in the 550–695°C range, which is due to the combustion of the coke deposited on the catalyst. Besides the weight loss, a slight weight gain caused by the oxidation of metallic Ni particles was also observed. The higher weight loss (45.9 wt%), centered at a temperature range of 584–689°C was observed for the 12COIMPNi11CoN-C sample after the reaction at 550°C, while this weight loss is about 5.8 wt% for the 4COIMPNi12LaN-C sample. But almost no weight loss was observed for the used samples in the reaction run at 700°C.

The DSC curves (see **Figure 9B**) of the samples show two exothermic peaks: (i) a small one at lower temperatures which can be assigned to oxidation of metallic nickel to Ni^{2+}; and (ii) a strong one at higher temperatures, which is due to the gasification of carbon. As the DSC curves present only one strong exothermic peak, one can conclude again that only one kind of carbon species was deposited on the surface of these catalysts, most likely graphite-like carbon.

Bimetallic Ni-Co/SBA-15 catalysts were considered as it has been proven that the addition of Co increases the basicity of catalysts and enhances the CO_2 adsorption, which effectively reduces the carbon deposition rate (Huang et al., 2015). As for the bimetallic Ni-La/SBA-15 catalysts, it has been found that the addition of a suitable amount of La as promoter increased the dispersion of NiO along with the interaction between NiO and silica support (Zhu et al., 2011).

CONCLUSIONS

In summary, an original method based on the analysis of the gas composition at the exit of the reactor, to predict, and monitor the carbon deposition during the dry reforming of the methane process over Ni-based catalysts, was proposed and tested on monometallic Ni/SBA-15 and bimetallic Ni-Co/SBA-15 and Ni-La/SBA-15 catalysts. As the prediction results were accurate when compared with the experimental ones, the method can be successfully used not only to predict whether the formation of coke is likely to occur but also to monitor the DRM process at different scales. The current research confirmed that the size of the Ni particles, which in turn depends on the nature of the nickel precursor and loading and on the preparation methods, is responsible for the coke formation: the smaller the size, the less probable the carbon deposition.

DATA AVAILABILITY STATEMENT

The raw data supporting the conclusions of this article will be made available by the authors, without undue reservation, to any qualified researcher.

AUTHOR CONTRIBUTIONS

RA performed most of the experimental work. TS contributed to the physical characterization of the samples. MO proposed the prediction method, analyzed the data, and wrote the paper. All authors contributed to the article and approved the submitted version.

SUPPLEMENTARY MATERIAL

The Supplementary Material for this article can be found online at: https://www.frontiersin.org/articles/10.3389/fceng.2020.00009/full#supplementary-material

REFERENCES

Ahmed, R. (2013). *High-efficiency catalysts for dry reforming of methane*. (PhD thesis). Teesside University, Middlesbrough, United Kingdom.

Akri, M., Zhao, S., Li, X., Zang, K., Lee, A. F., Isaacs, M. A., et al. (2019). Atomically dispersed nickel as coke-resistant active sites for methane dry reforming. *Nat. Commun.* 10:5181. doi: 10.1038/s41467-019-12843-w

Al-Fatish, A. S. A., Ibrahim, A. A., Fakeeha, A. H., Soliman, M. A., Siddiqui, M. R. H., and Abasaeed, A. E. (2009). Coke formation during CO_2 reforming of CH_4 over alumina-supported nickel catalysts. *Appl. Catal. A* 364, 150–155. doi: 10.1016/j.apcata.2009.05.043

Arbag, H., Yasyerli, S., Yasyerli, N., Dogu, G., and Dogu, T. (2016). Enhancement of catalytic performance of Ni based mesoporous alumina by Co incorporation in conversion of biogas to synthesis gas. *Appl. Catal. B Environ*. 198, 254–265. doi: 10.1016/j.apcatb.2016.05.064

Bengaard, H. S., Nørskov, J. K., Sehested, J., Clausen, B. S., Nielsen, L. P., Molenbroek, A. M., et al. (2002). Steam reforming and graphite formation on Ni catalysts. *J. Catal.* 209, 365–384. doi: 10.1006/jcat.2002.3579

Benrabaa, R., Löfberg, A., Caballero, J. G., Bordes-Richard, E., Rubbens, A., Vannier, R.-N., et al. (2015). Sol-gel synthesis and characterization of silica supported nickel ferrite catalysts for dry reforming of methane. *Catal. Comm.* 58, 127–131. doi: 10.1016/j.catcom.2014.09.019

Bradford, M. C. J., and Vannice, M. A. (1999). The role of metal-support interactions in CO_2 reforming of CH_4. *Catal. Today* 50, 87–96. doi: 10.1016/S0920-5861(98)00465-9

Edwards, J. H., and Maitra, A. M. (1995). The chemistry of methane reforming with carbon dioxide and its current and potential applications. *Fuel Proces. Technol.* 42, 269–289. doi: 10.1016/0378-3820(94)00105-3

Erdogan, B., Arbag, H., and Yasyerli, N. (2018). SBA-15 supported mesoporous Ni and Co catalysts with high coke resistance for dry reforming of methane. *Int. J. Hydrogen Energy* 43, 1396–1405. doi: 10.1016/j.ijhydene.2017.11.127

Guczi, L., Stefler, G., Geszti, O., Sajó, I., Pászti, Z., Tompos, A., et al. (2010). Methane dry reforming with CO_2: A study on surface carbon species. *Appl. Catal. A General* 375, 236–246. doi: 10.1016/j.apcata.2009.12.040

Han, J. W., Park, J. S., Choi, M. S., and Lee, H. J. (2017). Uncoupling the size and support effects of Ni catalysts for dry reforming of methane. *Appl. Catal. B Environ.* 203, 625–632. doi: 10.1016/j.apcatb.2016.10.069

Huang, T., Huang, W., Huang, J., and Ji, P. (2015). High stability of Ni-Co/SBA-15 catalysts for CH_4 reforming with CO_2. *Energy Sourcest A Recov. Util. Environ. Eff.* 37, 510–517. doi: 10.1080/15567036.2011.585387

Hukkamäki, J., Suvanto, S., Suvanto, M., and Pakkanen, T. T. (2004). Influence of the pore structure of MCM-41and SBA-15 silica fibers on atomic layer chemical vapor deposition of cobalt carbonyl. *Langmuir* 20, 10288–10295. doi: 10.1021/la048610q

Lin, H.-P., Tang, C.-Y., and Lin, C.-Y. (2002). Detailed structural characterization of SBA-15 and MCM-41 mesoporous silicas on a high-resolution transmission electron microscope. *J. Chin. Chem. Soc.* 49, 981–988. doi: 10.1002/jccs.200200140

Liu, D. P., Quek, X. Y., Cheo, W. N. E., Lau, R., Borgna, A., and Yang, Y. H. (2009a). MCM-41 supported nickel-based bimetallic catalysts with superior stability during carbon dioxide reforming of methane: effect of strong metal-support interaction. *J. Catal.* 266, 380–390. doi: 10.1016/j.jcat.2009.07.004

Liu, D. P., Quek, X. Y., Wah, H. H. A., Zeng, G. M., Li, Y. D., and Yang, Y. H. (2009b). Carbon dioxide reforming of methane over nickel-grafted SBA-15 and MCM-41 catalyst. *Catal. Today* 148, 243–250. doi: 10.1016/j.cattod.2009.08.014

Marceau, E., Che, M., Cejka, J., and Zukal, A. (2010). Nickel (II) nitrate vs. acetate: influence of the precursor on the structure and reducibility of Ni/MCM-41 and Ni/Al-MCM-41 catalysts. *ChemCatChem* 2, 413–422. doi: 10.1002/cctc.200900289

Nikolla, E., Schwank, J., and Linic, S. (2007). Promotion of the long-term stability of reforming Ni catalysts by surface alloying. *J. Catal.* 250, 85–93. doi: 10.1016/j.jcat.2007.04.020

Olea, M., Hodgson, S. N., and Ahmed, R. A. (2014). Metal catalysts supported on mesoporous material. *WO 2014/125309 A3*. Available online ta: https://patentscope2.wipo.int/search/en/detail.jsf;jsessionid$=$F64242B3B2D9A69E76E58AAB90F8EDD7?docId$=$WO2014125309&tab$=$PCTDESCRIPTION

San José-Alonso, D., Illán-Gómez, M. J., and Román-Martínez, M. C. (2013). Low metal content Co and Ni alumina supported catalyst for CO_2 reforming of methane. *Int. J. Hydrogen Energy* 38, 2230–2239. doi: 10.1016/j.ijhydene.2012.11.080

Steinhauer, B., Kasireddy, M. R., Radnik, J., and Martin, A. (2009). Development of Ni-Pd bimetallic catalysts for the utilization of carbon dioxide and methane by dry reforming. *Appl. Catal. A General* 366, 333–341. doi: 10.1016/j.apcata.2009.07.021

Tsai, H.-L., and Wang, C.-S. (2008). Thermodynamic equilibrium prediction for natural gas dry reforming in thermal plasma reformer. *J. Chinese Inst. Eng.* 31, 891–896. doi: 10.1080/02533839.2008.9671444

Verykios, X. E. (2003). Catalytic dry reforming of natural gas for the production of chemicals and hydrogen. *Int. J. Hydrogen. Energ.* 28, 1045–1063.

Xu, B. Q., Wei, J. M., Wang, H. Y., Sun, K. O., and Zhu, Q. M. (2001). Nano-Mg: novel preparation and applications support of Ni catalyst for CO_2 reforming of methane. *Catal. Today* 68, 217–225. doi: 10.1016/S0920-5861(01)00303-0

Zhao, D., Feng, J., Huo, Q., Melosh, N., Fredrickson, G. H., Chmelka, B. F., et al. (1998a). Triblock copolymer syntheses of mesoporous silica with periodic 50 to 300 angstrom pores. *Science* 279, 548–552. doi: 10.1126/science.279.5350.548

Zhao, D., Huo, Q., Feng, J., Chmelka, B. F., and Stucky, G. D. (1998b). Nonionic triblock and star diblock copolymer and oligomeric surfactant synthesis of highly ordered, hydrothermally stable, mesoporous silica structures. *J. Amer. Soc.* 120, 6024–6036. doi: 10.1021/ja974025i

Zhu, J. Q., Peng, X. X., Yao, L., Shen, J., Tong, D. M., and Hu, C. W. (2011). The promoting effect of La, Mg, Co and Zn on the activity and stability of Ni/SiO_2 catalyst for CO reforming of methane. *Int. J. Hydrogen Energy* 36, 7094–7104. doi: 10.1016/j.ijhydene.2011.02.133

Conflict of Interest: The authors declare that the research was conducted in the absence of any commercial or financial relationships that could be construed as a potential conflict of interest.